Early sorting of inner nuclear membrane proteins is conserved

Sharon C. Braunagel*, Shawn T. Williamson†, Qi Ding*, Xiaogiang Wu*, and Max D. Summers*†‡§¶

*Texas Agricultural Experiment Station, Departments of †Biology, ‡Entomology, and §Biochemistry and Biophysics, Texas A&M University, College Station, TX 77843

Contributed by Max D. Summers, April 10, 2007 (sent for review January 3, 2007)

***Spodoptera frugiperda* (Sf9) importin-α-16 is a translocon-associated protein that participates in the early sorting pathway of baculovirus integral membrane proteins destined for the inner nuclear membrane (INM). To discern whether sorting intermediate protein complexes like those observed in insect cells are also formed with mammalian INM proteins, cross-linked complexes of importin-α-16 with human lamin B receptor (LBR) and nurim were examined. Both LBR and nurim cross-link with Sf9 importin-α-16 during cotranslational membrane integration and remain proximal with importin-α-16 after integration into the endoplasmic reticulum membrane and release from the translocon. Human cells encode several isoforms of importin-α; to determine whether any of these isoforms may recognize INM-directed proteins, they were tested for their ability to cross-link with the viral-derived INM sorting motif sequence. One cross-linked adduct was detected with a 16-kDa isoform encoded from *KPNA4* (KPNA-4–16). KPNA-4–16 was easily detected in microsomal membranes prepared from *KPNA4–16* recombinant virus-infected cells and was also detected in microsomes prepared from HeLa cells. Together these observations suggest that elements of the early sorting pathway of INM-directed proteins mediated by importin-α-16 are highly conserved, and mammalian KPNA-4–16 is a candidate partner in sorting integral membrane proteins to the INM.**

importin-α | protein trafficking | kapα | nucleus

Although much is known about the mechanism of transport of soluble proteins through the nuclear pore complex (NPC), the mechanism used by integral membrane proteins during their transit from the endoplasmic reticulum (ER) to the inner nuclear membrane (INM) is not yet resolved. One proposed mechanism is that INM-directed proteins diffuse by random walk along the continuous membranes of the ER, outer nuclear membrane (ONM), pore membrane, and INM, and at the INM they are retained by binding with nucleoplasmic ligands (1). However, recent data from several laboratories show that trafficking of INM proteins from the ER to the INM involves more than lateral diffusion. We now know that trafficking of integral membrane proteins to the INM may require energy (2) and be mediated by multiple protein interactions (3–6).

Recognition and sorting of INM-directed proteins can begin during cotranslational membrane integration in the ER (4). Using a baculovirus-derived amino acid sequence sufficient to target fusion proteins to the INM-sorting motif (INM-SM), a cellular protein participating in this process has been identified (5). This protein is a small, membrane-associated isoform of importin-α, importin-α-16, which is positioned in the ER membrane in close proximity to the translocon protein, Sec61α, and recognizes INM-directed proteins while their nascent chain is inserted in the translocon and bound to the ribosome. Importin-α-16 remains closely associated with the INM-directed proteins after ER membrane integration (5).

In this study, we show that human LBR and nurim cross-link with *Spodoptera frugiperda* (Sf9) importin-α-16 during cotranslational membrane integration, and importin-α-16 remains in close proximity with these proteins after they integrate into the ER membrane. Human cells encode several small isoforms of human importin-α, and a cross-linked adduct with the viral INM-SM sequence can be detected with a 16-kDa isoform encoded from *KPNA4* (KPNA-4–16). KPNA-4–16 is readily detected in microsomal membranes prepared from recombinant virus-infected cells and can be detected in microsomal membranes prepared from HeLa cells. These observations suggest that elements of the early sorting pathway of INM-directed proteins are conserved and transcend species boundaries.

Results

The first goal of this study was to determine whether resident proteins of the mammalian INM form transient-intermediate protein complexes similar to those identified with the viral-derived INM-SM in insect cells (5). Before proceeding with directed cross-linking assays, two determinants had to be established for LBR. To generate correct LBR-fusion constructs, the features of LBR that regulate its orientation in the ER membrane had to be identified. With this knowledge, an LBR substrate for use with the soluble, lysine-specific cross-linking reagent BS^3 (11.4-Å spacer arm) could be generated. To determine whether Sf9 cell-derived microsomal membranes are a valid membrane substrate for these studies, we needed to confirm that LBR is correctly targeted to the INM in Sf9 cells. The advantage of using insect cell-derived microsomal membranes for *in vitro* translation/cross-linking assays is that they can be loaded with an appropriate bait protein by using recombinant baculoviruses (3, 5). In this way, cross-linking assays can be performed that directly test the interaction of two known proteins with defined substrate lysines.

Determinants for Orientation of LBR Reside Within the N-Terminal, Cytoplasmic Domain. To determine the structural domains that regulate the orientation of LBR in the ER membrane, an *in vitro* glycosylation assay was used (7). The data showed that the N-terminal region of LBR was essential for properly orienting LBR in the ER membrane [supporting information (SI) Fig. 6]. Subsequent experiments were performed by using the N-terminal LBR sequence through TM1 ($LBR_{1–238}$).

LBR Is Directed to the INM in Sf9 Cells and Is Mobile in That Location. To discern whether LBR was correctly sorted to the INM in insect cells, $LBR_{1–238}$GFP was transiently expressed in Sf9 cells and its location was determined by using confocal microscopy

Author contributions: S.C.B. and Q.D. designed research; S.C.B., S.T.W., Q.D., and X.W. performed research; S.T.W. and Q.D. contributed new reagents/analytic tools; M.D.S. analyzed data; and S.C.B. wrote the paper.

The authors declare no conflict of interest.

Freely available online through the PNAS open access option.

Abbreviations: ER, endoplasmic reticulum; FRAP, fluorescent recovery after photobleaching; INM, inner nuclear membrane; INM-SM, INM-sorting motif; LBR, lamin B receptor; NLS, nuclear localization sequence; NPC, nuclear pore complex; ONM, outer nuclear membrane.

¶To whom correspondence should be addressed. E-mail: m-summers@tamu.edu.

This article contains supporting information online at www.pnas.org/cgi/content/full/0703186104/DC1.

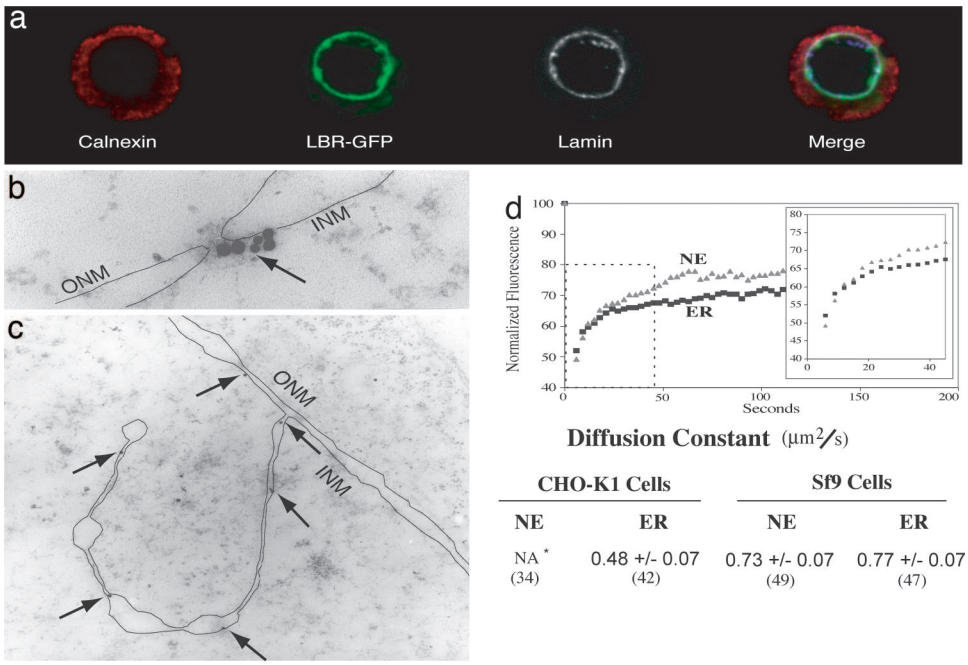

Fig. 1. Cellular localization of $LBR_{1–238}GFP$ transiently expressed in Sf9 cells. (*a*) Confocal microscopy images of $LBR_{1–238}GFP$. A single z-section is shown. Calnexin labeling is red, $LBR_{1–238}GFP$ is green, and lamin Dm0 is white. For ease of viewing, lamin Dm0 is recolored in blue in the merge image. (*b* and *c*) Sf9 cells transiently expressing $LBR_{1-238}GFP$ were fixed, thin sectioned, and analyzed by using GFP antibody and 25 nM gold-conjugated secondary antibody. The membranes are outlined, ONM and INM are labeled, and arrows point to the location of $LBR_{1–328}GFP$. (*d*) FRAP was used to determine recovery kinetics of $LBR_{1–238}GFP$ in CHOK1 and Sf9 cells. (*Upper*) A graphical recovery curve of $LBR_{1–138}GFP$ in Sf9 cells. (*Lower*) Calculated diffusion constants for the complete analyses. Total sample size is listed in parentheses.

and antibodies to the marker proteins calnexin (bulk ER) and lamin Dm0 (nuclear boundary). $LBR_{1–238}GFP$ was detected as a bright ring of fluorescence surrounding the nucleus, and the merged image shows that $LBR_{1–238}GFP$ colocalized with lamin (Fig. 1*a*). Immunogold-labeled cells transiently expressing $LBR_{1–238}GFP$ were analyzed to determine whether LBR was located in the ONM or INM. $LBR_{1–238}GFP$ was detected closely associated with the inner side of the nuclear pore (Fig. 1*b*) and in the INM (Fig. 1*c*). Consistent with previous results, it was common to observe invaginations of the INM into the nucleoplasm (8). An example of such an invagination is shown in Fig. 1*c*, and $LBR_{1–238}GFP$ was easily detected in these regions (Fig. 1*c*, arrows). Thus, during transient expression in Sf9 cells, $LBR_{1–238}GFP$ accumulates in the INM.

Fluorescent recovery after photobleaching (FRAP) assays performed with LBR, emerin, MAN1, and nurim show that, once located at the INM of mammalian cells, these proteins have limited mobility (8–11). To determine whether LBR was immobilized in the INM in Sf9 cells, we also used FRAP. As a control, recovery kinetics of $LBR_{1–238}GFP$ expressed in the mammalian cell line, CHO-K1, were determined. In these cells, $LBR_{1–238}GFP$ at the nuclear rim had limited mobility, whereas protein located in the ER was mobile (Fig. 1*d*). In contrast, when expressed in Sf9 cells, $LBR_{1–238}GFP$ had approximately equal and high mobility in the ER and nuclear membrane (Fig. 1*d*). Thus, in Sf9 cells, the accumulation of $LBR_{1–238}GFP$ in the INM was not due to immobilization.

LBR Is Proximal to Sf9 Importin-α-16 During Translation and After ER Membrane Integration. We know that the lysine–lysine cross-linking reagent BS^3 can covalently link Sf9 importin-α-16 with the viral-derived INM-SM sequence (5). To generate an appropriate LBR cross-linking substrate, the lysines in the N-terminal region of LBR were replaced with arginine (SI Fig. 6*b*), and the mutated sequence was fused to the lysine-free cassette described previously (3). In the clone LBR-ΔK, only $lysine_{205}$ was available as a substrate for BS^3 (Fig. 2*a*). Because previous data show that optimal placement to the positively charged amino acid in the INM-SM sequence is 5–8 amino acids from the end of the TM sequence, a second clone was generated that replaced $arginine_{203}$ with lysine (LBR-KΔK; Fig. 2*a*).

When radiolabeled LBR-KΔK was translated in the presence of microsomal membranes containing Sf9 importin-α-16-T7 and exposed to BS^3 (Fig. 2*b*), a cross-linked adduct at an appropriate molecular mass was enriched on the His-binding TALON-beads (Fig. 2*e*, lane 2, *) or was precipitated by using T7 antibody (Fig. 2*e*, lane 3, *). The cross-linked adduct was not detected if BS^3 was omitted or precipitation was performed by using mouse IgG (Fig. 2*e*, lanes 1 and 4, respectively).

Previous results show that the viral INM-SM sequence cross-links with importin-α-16 while the nascent chain is inserted in the translocon and bound to the ribosome (5). Thus, the next experiment was designed to discern whether LBR-KΔK would also cross-link with importin-α-16-T7 during cotranslational membrane integration. For this experiment, a truncated mRNA of LBR-KΔK lacking the stop codon was generated and translated in the presence of microsomes containing Sf9 importin-α-16-T7 and exposed to BS^3 (Fig. 2*c*). A TALON-enriched, cross-linked adduct at the appropriate molecular mass was detected (Fig. 2e, lane 5, *).

To test whether ER membrane-integrated LBR would cross-link with newly translated importin-α-16, radiolabeled importin-α-16-T7 was translated in the presence of microsomal membranes preloaded with LBR-KΔK (Fig. 2*d*) and then exposed to BS^3. The $(His)_7$ tag in the preloaded, nonradiolabeled LBR-KΔK was used to enrich the cross-linked adduct (Fig. 2*d*). A cross-linked adduct at the appropriate molecular weight was detected (Fig. 2*e*, lane 7, *). A decreased amount of cross-linked adduct was detected compared with the reciprocal experiment (compare lanes 2–3 with lane 7). It is possible that preloaded

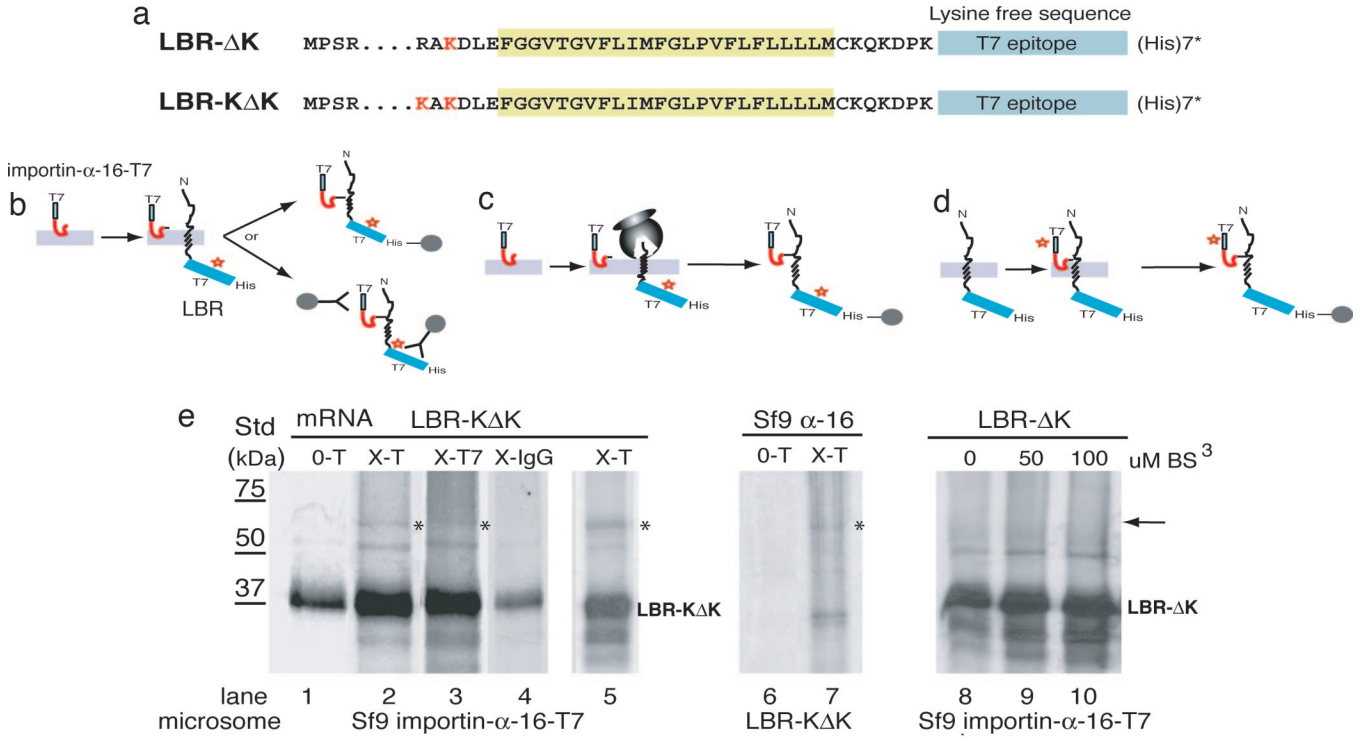

Fig. 2. LBR amino acid 203 is proximal to Sf9 importin-α-16. (*a*) The lysines in $LBR_{1–238}$ were changed to arginine (SI Fig. 6*b*) and then fused to a lysine-free sequence. The lysines available as cross-linking substrates are highlighted in red, transmembrane sequences are highlighted in yellow, and the lysine-free cassette containing the T7 epitope is highlighted in blue. (*b–d*) Schematics illustrate experimental protocol used in *e*. The protein marked with the red star is radiolabeled in the assay. *b* corresponds to the protocol used to generate data shown in lanes 1–4 and 8–10, *c* was used for lane 5, and *d* was used for lanes 6 and 7. (*e*) Radiolabeled LBR-KΔK was translated in the presence of microsomal membranes containing Sf9 importin-α-16-T7. The cross-linked adduct enriched on TALON beads is shown in lane 2 (*) while lane 3 shows the adduct precipitated by using T7 antibody (*). Lane 1 shows TALON-enriched product after treatment with buffer alone. The data presented in lanes 1–4 are from the same exposure of a single gel. To ensure that negative data shown in lane 1 are not due to a decreased quantity of enriched LBR-KΔK, the gel was exposed for a longer period, and the cross-linked adduct was not detected (data not shown). Lane 4 shows that the cross-linked adduct was not precipitated by using normal mouse IgG. Lane 5 shows the results of translation and cross-linking of truncated LBR-KΔK, and the cross-linked adduct is indicated (*). In lanes 6 and 7, radiolabeled Sf9 importin-α-16-T7 was translated in the presence of membranes containing LBR-KΔK, and the cross-linked adduct enriched on TALON beads is noted (*). In lanes 8–10, radiolabeled LBR-ΔK was translated in the presence of membranes containing Sf9 importin-α-16-T7 and exposed to buffer alone (lane 8); 50 or 100 μM BS^3 (lanes 9 and 10) and the membrane pellet were analyzed. The arrow indicates the molecular mass of the expected cross-linked complex.

LBR-KΔK was already bound to endogenous importin-α-16 and, as such, only a limited quantity of LBR-KΔK was available for binding with newly presented, radioactive importin-α-16.

To test whether the optimally positioned $lysine_{203}$ is responsible for cross-linking with importin-α-16, the cross-linking experiments were repeated by using radiolabeled LBR-ΔK (Fig. 2*a*). A cross-linked adduct was not detected (Fig. 2*e*, lanes 8–10, arrow). Thus, the cross-linked adduct detected by using LBR-KΔK was due to the proximal positioning of $lysine_{203}$ and importin-α-16-T7.

Nurim Is Proximal to Sf9 Importin-α-16 During Translation and After ER Membrane Integration. Like LBR, nurim is a polytopic protein that accumulates and has limited mobility in the INM (10). Nurim has few amino acids exposed within the cytoplasm or nucleoplasm (12), and there is no evidence that nurim binds to lamins, nuclear pores, or other nucleoplasmic components (10). Mutations made throughout the gene decrease protein accumulation in the INM. As such, it is postulated that: (*i*) nurim binds to another INM protein and this interaction directs its destination, and/or (*ii*) nurim acts as an integrated structure and various mutations alter the presentation of critical targeting/binding sequences (10).

The cytoplasmic loops between TM2-TM3 and TM4-TM5/6 contain conserved lysines that fulfill the requirements of the INM-SM sequence (SI Fig. 7), and, as such, cross-linking assays could be performed without generating directed-mutations. Nurim cross-linking experiments were performed by using two mRNAs: (*i*) full-length nurim mRNA, and (*ii*) a truncated mRNA that lacks the stop codon. Both mRNAs were radiolabeled and translated in the presence of microsomes containing importin-α-16-T7, exposed to BS^3, and either enriched by using TALON beads or precipitated by using T7 antibody (Fig. 3 *a* and *b*). A cross-linked importin-α-16 adduct was detected when both full-length (Fig. 3*c*, lanes 2–4, *) and truncated nurim mRNAs were translated (Fig. 3*c*, lanes 6–7, *). Thus, like LBR and the viral INM-SM, nurim is proximal to importin-α-16 while associated with the ribosome and translocon and remains with importin-α-16 after it is integrated into the ER membrane.

Mammalian Cells Have a Counterpart to Sf9 Importin-α-16 and It Cross-Links with the Viral INM-SM Sequence. The ability of LBR and nurim to cross-link with Sf9 importin-α-16 demonstrates that the same pathway described for the viral INM-SM may also facilitate sorting of mammalian integral membrane proteins to the INM. Thus, the second goal of this study was to determine whether human importin-α genes encode an importin-α-16-like protein. To achieve this goal, primer extension analyses were performed with all six human genes (*KPNA1–6*), and four transcripts were

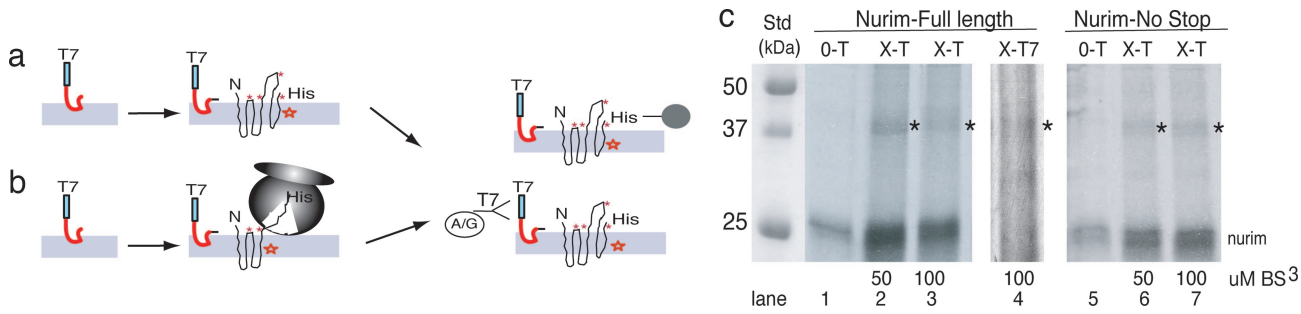

Fig. 3. Nurim is proximal to Sf9 importin-α-16 both during and after cotranslational membrane integration. (*a* and *b*) Schematic illustrating the experimental design used for the data presented in *c*. Nurim is radiolabeled in these assays, and this is noted in the schematic with a red star. (*c*) Full-length (lanes 1–4) or truncated nurim (lanes 5–7) were translated in the presence of microsomal membranes containing Sf9 importin-α-16-T7 and exposed to buffer alone (lanes 1 and 5) or two concentrations of BS^3 (noted below gel). The reaction was either treated with TALON beads (lanes 1–3, 5–7) or precipitated by using T7 antibody (lane 4). The exposure was increased for the T7 antibody precipitated lane. The cross-linked adduct is noted (*).

detected. The full primer extension analyses of the KPNA genes and predicted importin-α isoforms are described in SI Figs. 8–11.

To discern whether any of the mammalian importin-α isoforms recognize the INM-SM, all were tested in cross-linking assays with the viral INM-SM protein. For these experiments, the KPNA constructs were tagged at the C terminus with the T7 epitope, radiolabeled, and translated in the presence of microsomal membranes preloaded with the viral INM-SM cassette (5). To ensure that cross-linked adducts were not missed, total membranes samples were analyzed. A 16-kDa protein predicted from a transcript of *KPNA4* (KPNA-4–16) was the only isoform forming a detectable cross-linked adduct (Fig. 4*a*), and this adduct could be precipitated by using T7 antibody (data not shown). KPNA4–16 contains ARM 8 to the C terminus of KPNA4 (SI Figs. 8 and 11).

KPNA-4–16 Is Present in Microsomal Membranes. Both T7-epitope-tagged *KPNA-4–26* (a larger isoform encoded from *KPNA4*; see SI Figs. 8 and 11) and *KPNA-4–16* were expressed in Sf9 cells by using recombinant baculoviruses. When *KPNA-4–26* was expressed, both KPNA-4–26 and KPNA-4–16 were detected (Fig. 4*b*, lane 1; compare this result with lane 2, which shows only expression of *KPNA-4–16*). When microsomal membranes were prepared from cells infected with recombinant virus-expressing T7-tagged *KPNA-4–16*, the T7 antibody easily detected KPNA-4–16. However, it detected two forms of the protein, one with a slightly smaller molecular mass (Fig. 4*b*, lane 3). These data show that KPNA-4–16 locates to microsomal membranes and suggests that one form may be modified in such a way that its migration pattern on SDS/PAGE gels is altered. To test the reactivity of the KPNA4-specific antibody (generated to a C-terminal epitope; described in SI Fig. 11), a matched sample of recombinant virus-derived microsomal membranes was analyzed by using this antibody. Compared with the T7 antibody, the KPNA-4 specific antibody only detected faint bands corresponding to KPNA-4–16 in these microsomes (compare Fig. 4*b*, lanes 3 and 4; see legend for exposure times). When microsomes prepared from HeLa cells were analyzed, the KPNA4-specific antibody detected bands corresponding to KPNA4–16 (Fig. 4*b*, lane 5). We note that KPNA4–16 is not readily detected in total cell lysates (data not shown) or in fractions containing enriched, intact nuclei (Fig. 4*b*, lane 6).

Discussion

FRAP and kinetic calculations thereof have strongly supported the diffusion-retention model for INM-directed protein trafficking. However, recent analyses reveal that traditional FRAP calculations can miss transient protein interactions, and complementary biochemical methods are required to detect them (12). A more thorough understanding of the multiple forces that come into play in a traditional FRAP experiment may help reconcile the apparently contradictory models of INM-directed protein trafficking of diffusion retention versus an active mechanism mediated by multiple protein interactions.

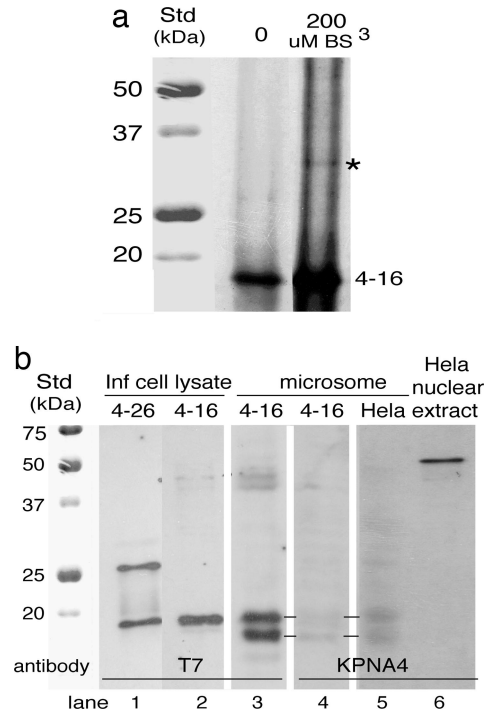

Fig. 4. KPNA-4–16 cross-links with INM-SM and is present in microsomal membranes. (*a*) KPNA-4–16 was translated in the presence of microsomal membranes containing the viral INM-SM cassette, treated with buffer or 200 μM BS^3, and membrane pellet-resolved by using SDS/PAGE. The cross-linked sample is noted (*). (*b*) Recombinant virus-infected cell extracts (30 μg per lane) were analyzed (*KPNA-4–26-T7*, lane 1; *KPNA-4–16-T7*, lane 2). A KPNA-4–16 isoform was detected when the slightly larger *KPNA-4–26* gene was expressed. Microsomal membranes were prepared from *KPNA-4–16-T7*-infected cells, and KPNA-4–16 was easily detected by using T7 antibody (lane 3; 30-sec exposure; 30-eq microsomal membranes); however, two forms were detected. When a matched sample probed with KPNA-4-specific antibody was analyzed (compare lanes 3 and 4), substantially less positive product was detected (lane 4; 5-min exposure). KPNA4 antibody detected KPNA-4–16 in microsomal membranes prepared from HeLa cells (lane 5; 15-min exposure; 30-eq microsomal membranes), whereas no cross-reactivity was detected in microsomes prepared from Sf9 or wild-type baculovirus-infected cells (data not shown). KPNA-4–16 was not detected when analyzing total cell extracts (data not shown) or extracts of enriched nuclei (120 μg; lane 6).

Regardless of the mechanism of INM-directed protein trafficking, protein-ligand interactions that occur once the protein resides within the INM predict decreased mobility (1). Thus, the FRAP result showing that human LBR was mobile in the INM of Sf9 cells was unexpected. Although Sf9 LBR has not been identified, the *Drosophila melanogaster* ortholog of human LBR (dLBR) has been characterized. The N-terminal region of dLBR binds to the insect lamin Dm0; however, binding of dLBR and Dmo is not essential for accumulation of dLBR in the INM (13). This is in contrast to other insect INM proteins (dMAN1, Bocksbeutel, and otefin), whose INM localizations are directly influenced by the presence of insect lamin Dm0 (14). Together these data suggest that sorting of dLBR to the INM does not depend solely on immobilizing protein–protein interactions occurring at the INM. Thus, LBR expressed in insect cells may provide an ideal substrate for dissection of intermediate stages of sorting of INM-directed integral membrane proteins.

Insect and Mammalian Cells Share Common Features of INM-Directed Protein Sorting. The INM-SM sequence was initially discovered within an envelope protein of baculovirus. The motif includes two major features: (*i*) a hydrophobic stretch of 18–20 amino acids that constitute a transmembrane sequence, and (*ii*) positively charged residues exposed within the cyto/nucleoplasm positioned within 4–8 amino acids from the end of the transmembrane sequence (3). A comparison of events occurring during the first stage of interaction between the TM sequences within the INM-SM and the translocon shows that TM sequences of INM-directed proteins occupy a similar binding site within the translocon, and this site differs from that occupied by non-INM-directed proteins(4).

The viral INM-SM sequence constitutes a noncleaved, type-1 signal anchor (15). Because no other INM protein utilizes such an anchor for membrane integration, it was initially difficult to predict whether sorting events deciphered for the viral INM-SM would be relevant for other INM-directed proteins. The results presented here support the proposal that the sorting pathway identified with the viral-derived INM-SM in insect cells is also directing other integral membrane proteins to the INM. Human LBR and nurim cross-link with Sf9 importin-α-16, and both of these proteins are proximal to importin-α-16, while their nascent chains are bound to the ribosome and inserted in the translocon. These data suggest that, like in insects, recognition and sorting of mammalian INM-directed proteins can be initiated at the time of cotranslational membrane integration.

Mammalian cells generate multiple transcripts that predict the existence of truncated isoforms of importin-α. A unique transcript predicting KPNA-4–16 is present, and KPNA-4–16 can be generated from *KPNA-4–26*. These data suggest that KPNA-4–16 can either be generated from an independent transcript encompassed with *KPNA-4–26* (which is only 280 nt larger than the transcript encoding KPNA-4–16) or be a result of an alternate translation initiation from the internal methionine. Cross-linking with the INM-SM was only detected with KPNA-4–16. KPNA-4–16 could be detected in ER-enriched microsomal membranes prepared from recombinant virus-infected or HeLa cells.

An Integrated Model of INM-Directed Protein Trafficking. It is now possible to integrate observations of INM-directed protein trafficking generated from several laboratories into a unified model (Fig. 5). The data suggest that importin-α-16 (or KPNA-4–16) functions early in the sorting pathway. It resides in the ER membrane in close proximity to the translocon protein Sec 61α (Fig. 5*a*), thus appropriately positioning it to survey, discriminate, and bind with INM-directed nascent chains as they make contact with the translocon (Fig. 5*b*). After integration into the ER membrane, the INM-directed protein is proximal to

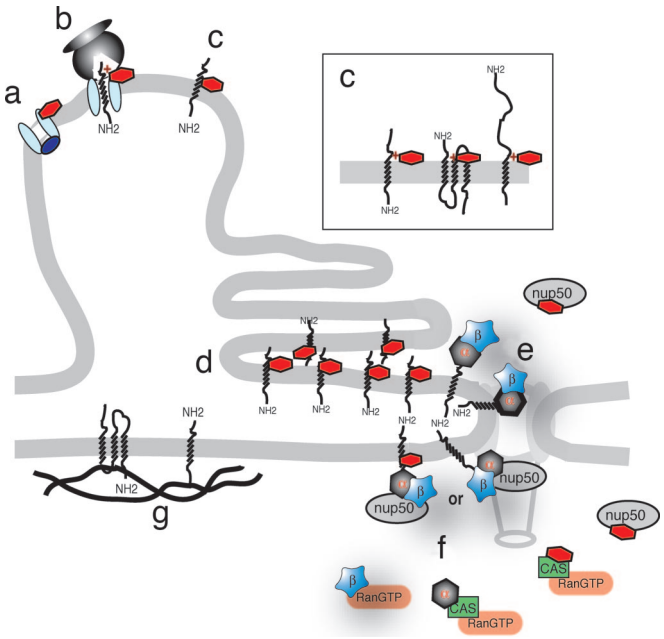

Fig. 5. Integrated model of directed trafficking of INM proteins. (*a*) Membrane associated importin-α-16 (KNPA-4–16) resides proximal to Sec61α. (*b*) During cotranslational membrane integration, INM-directed proteins are proximal to importin-α-16. (*c*) Importin-α-16 remains with the INM-directed proteins after ER membrane integration. INM-directed proteins can also associate with importin-α-16 after membrane integration. Thus, the class of mature protein does not appear to matter relative to INM protein-importin-α-16 interaction (*Inset*). (*d*) INM-directed proteins concentrate in membranes closely associated with the nucleus. (*e*) NLS sequences of INM-directed proteins form complexes with importins-α and -β and are translocated across the nuclear pore. (*f* and *g*) INM protein complexes disassemble (*f*) and interact (*g*) with their nucleoplasmic ligands.

importin-α-16 (Fig. 5*c*). Cross-linking experiments show that an ER membrane-integrated INM-directed protein will also cross-link with importin-α-16 posttranslationally (Fig. 2*e*, lane 7, and Fig. 4*a*) (5). Although speculative, such posttranslational association of the INM-directed protein and KPNA-4–16 this may explain how INM-directed proteins with C-terminal anchors (e.g., emerin and lap2-β), which are integrated into the ER membrane in a posttranslational manner, may be incorporated into a common INM-directed targeting pathway mediated by importin-α-16-like proteins. The interaction of the INM-protein and importin-α-16 occurs through the appropriately positioned, positively charged amino acid in the INM-SM-like sequence exposed on the cytoplasmic face of the ER membrane. In this way, the interaction is independent of the class assignment of the mature INM protein (type I, II, etc.; Fig. 5*c Inset*). These events in the sorting pathway do not seem to be related to any size-selective barrier potentially imposed by the NPC.

The observation that importin-α-16 can bind to and remain with the INM-directed protein after membrane integration suggests that its function continues past cotranslational membrane integration. Recent observations suggest a function for this complex. When the nuclear localization sequence (NLS) of the yeast protein Heh2 was mutated or expressed in *NUP2*- or *NUP170*-null mutants, Heh2 accumulated in membrane stacks closely associated with the ONM (6). These observations show that forces driving the lateral movement of Heh2 from the peripheral ER toward the ONM are independent of NLSs, nup2p or nup170p, and precede nuclear pore translocation. Using the insect model, we have shown that when the INM-SM sequence is altered, protein is redistributed from the nuclear rim to the peripheral ER (3). Thus, one role of importin-

α-16-mediated sorting may be to concentrate INM-directed proteins in membranes in close proximity to the nuclear periphery (Fig. 5*d*). As predicted by King *et al.* (6), once positioned at the NPC, the INM-directed protein undergoes NLS-mediated protein interactions (Fig. 5*e*), and importin-α (and possibly importin-β) facilitates translocation across the NPC. At the INM, the NLS-α–NLS-β complex disassociates and releases the INM-directed protein (Fig. 5*f*), allowing it to bind with its nuclear ligand (Fig. 5*g*).

The prior model incorporates many existing observations, but not all of them. Gerace and colleagues (2) show that INM-directed protein transport requires ATP, yet where in the pathway ATP is consumed versus utilization of the RAN cycle is unknown. Gp210 has been implicated in this pathway, but its role is unknown (2). If the function of importin-α-16 (or KPNA-4–16) is to sort and concentrate INM-directed proteins in the ONM, there must be additional proteins that facilitate this directed, lateral trafficking, yet their identity remains elusive.

As with any new area of study, the implications of understanding the mechanism of transport to the INM for such an important class of integral membrane proteins can only be speculated at this time. However, considering the role of these proteins in human disease, a more comprehensive understanding of the full range of functional interactions in this trafficking pathway should not only expand our understanding of these disease states, but also increase the opportunities to intervene in their progression.

Materials and Methods

Gene Constructs/Preparation of Microsomal Membranes/LBR Orientation. The construct $LBR_{1–238}$GFP (pEGFP-N1; CMV promoter) has been described (8). For insect cell expression, $LBR_{1–238}$GFP was cloned into pIE1–4 (Novagen, Madison, WI). The techniques used for LBR orientation analyses are described in SI Fig. 6. Sf9-derived microsomal membranes were isolated as reported (4).

Transient Expression/Confocal and EM. Transient expression was performed by using the calcium phosphate method as described (16). The cells were prepared for microscopy at 48 h posttransfection as described (17). Slides were viewed by using a Zeiss Axiovert 135 with a CARV confocal module (Carl Zeiss, Thornwood, NY). Representative cells were acquired by using Zeiss Axiovision 3.1 collected at 0.75-μm intervals. Antibodies used were calnexin CT (1:1,000; Stressgen, Victoria, BC, Canada), Adl67 (18) (1:250), and GFP (1:1,000; Molecular Probes Eugene, OR). Immunogold EM was performed as described (19).

FRAP. SF9 or CHO-K1 cells were transfected, seeded, and washed with serum-free media. FRAP was performed by using a Meridian Ultima Laser Confocal Microscope and Meridian software package (Image Analysis Laboratory; College of Veterinary Medicine, Texas A&M University). A 1.3-μm strip through the cell was bleached with scanning laser strength of 300 μWatts and bleaching laser strength of 2 mWatts. The area was scanned every 3 sec for 5 min. Lateral mobility was determined by using the method described (20). The data were analyzed with GraphPad (San Diego, CA) Instat 3 by using a *t* test (95% confidence interval).

Primer Extension Analysis. Transcript initiation was mapped by using the strand-specific oligonucleotide for each *KPNA* gene and primer extension technique as described (19,21) and shown in SI Figs. 7–10.

Translation and Cross-Linking. PCR-generated templates were used to transcribe mRNAs coding for nascent chains as described (4). After translation, microsomes were pelleted, and the membrane pellet was resuspended in BS^3 cross-linking buffer (3) and then split into control and cross-linked samples. BS^3 [Bis (sulfosuccinimidyl) suberate; Pierce, Rockford, IL] was used as the cross-linking reagent. Talon purification and immunoprecipitation were performed as described (4).

Western Blot. Antiserum against epitopes of KPNA 4 (1:2,000; Imgenex, San Diego, CA; shown in SI Fig. 11) and T7 (1:5,000; Novagen) were used.

We thank Jan Ellenberg (European Molecular Biology Laboratory, Heidelberg, Germany) for the 1–238 Lamin B Receptor EGFP construct, Melissa Rolls (University of Oregon, Eugene, OR) for the nurim clone, Paul Fisher (University of New York at Stony Brook, Stony Brook, NY) for ADL67 antiserum (*Drosophila* lamin), and Robert Burghardt and Rola Barhoumi-Mouneimne for their FRAP expertise and facilities. This work was supported by Texas Agricultural Experiment Station Project Grant TEXO-08078 (to M.D.S.). Portions of this manuscript were submitted by S.T.W. in partial fulfillment of the PhD degree at Texas A&M University.

1. Soullman B, Worman HJ (1995) *J Cell Biol* 130:15–27.
2. Ohba T, Schirmer EC, Nishimoto T, Gerace L (2004) *J Cell Biol* 167:1051–1062.
3. Braunagel SC, Williamson ST, Saksena S, Zhong S, Russell WK, Russell DH, Summers MD (2004) *Proc Natl Acad Sci USA* 101:8372–8377.
4. Saksena S, Shao Y, Braunagel SC, Summers MD, Johnson AE (2004) *Proc Natl Acad Sci USA* 101:12537–12542.
5. Saksena S, Summers MD, Burks JK, Johnson AE, Braunagel SC (2006) *Nat Struct Mol Biol* 13:500–508.
6. King MC, Lusk CP, Blobel G (2006) *Nature* 442:1003–1007.
7. Nilsson I, Saaf, W, Whitley P, Gafvelin G, Waller C, von Heijne G (1998) *J Mol Biol* 284:1165–1175.
8. Ellenberg J, Siggia ED, Moreira JE, Smith CL, Presley JF, Worman HJ Lippincott-Schwartz J (1997) *J Cell Biol* 138:1193–1206.
9. Wu W, Lin F, Worman HJ (2002) *J Cell Sci* 115:1361–1371.
10. Rolls MM, Stein PA, Taylor SS, Ha E, McKeon F, Rapoport TA (1999) *J Cell Biol* 146:29–44.
11. Ostlund C, Ellenberg J, Hallberg E, Lippincott-Schwartz J, Worman HJ (1999) *J Cell Sci* 112:1709–1719.
12. Beaudouin J, Mora-Bermúdez F, Klee T, Daigle N, Ellenberg J (2006) *Biophys J* 90:1878–1894.
13. Wagner N, Weber D, Seitz S, Krohne G (2004) *J Cell Sci* 117:2015–2028.
14. Wagner N, Kagermeier B, Loserth S, Krohne G (2006) *Eur J Cell Biol* 85:91–105.
15. Hong T, Summers, MD, Braunagel SC (1997) *Proc Natl Acad Sci USA* 94:4050–4055.
16. Summers MD, Smith GE (1987). *A Manual of Methods for Baculovirus Vectors and Insect Cell Culture Procedures* (Texas Agricultural Experiment Station, College Station, TX), Bulletin 1555.
17. Rosas-Acosta G, Braunagel SC, Summers MD (2001) *J Virol* 75:10829–10842.
18. Stuurman N, Sasse B, Fisher PA (1996) *J Struct Biol* 117:1–15.
19. Braunagel SC, Elton DM, Ma H, Summers MD (1996) *Virology* 217:97–110.
20. Yguerabide J, Schmidt JA, Yguerabide EE (1982) *Biophys J* 40:69–75.
21. Sambrook J, Fritsch EF, Maniatis T (1989) *Molecular Cloning: A Laboratory Manual* (Cold Spring Harbor Lab Press, Cold Spring Harbor, NY).